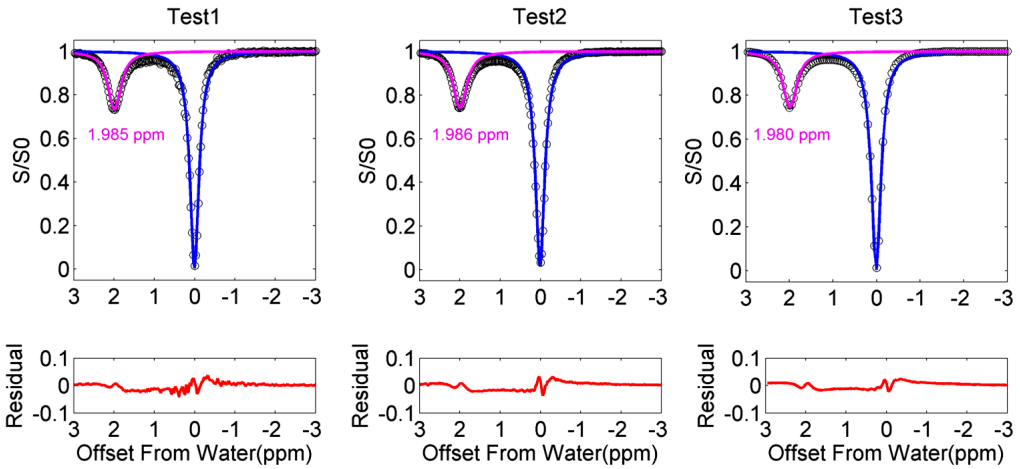

Figure S1 Raw and fitted Z-spectra of C0 phantom {[Cr] =40 mM, pH =7.2, and temperature =37 ℃} recorded on 3 different days with the same scan setup of 400 MHz NMR experiments. The apparent chemical shift, amplitude, linewidth, and the integral of CrCEST peaks were listed in *Table S1* in detail. The black circles represent the raw Z-spectra signals. The black, blue and pink lines represent the fitted Z-spectra, fitted spectra of the water pool, and fitted spectra of the Cr pool, respectively. Cr, creatine; NMR, nuclear magnetic resonance; CrCEST, CEST effect of Cr; CEST, chemical exchange saturation transfer.

Table S1 CrCEST peak parameters of the fitted Z-spectra of C0 phantom recorded on 3 different days in 400 MHz NMR experiments {[Cr] =40 mM, pH =7.2, and temperature =37 ℃}

CrCEST peak parameters	Apparent chemical shift (ppm)	Amplitude	Linewidth	Integral
Test 1	1.985	0.269	0.384	0.151
Test 2	1.986	0.261	0.399	0.152
Test 3	1.980	0.258	0.377	0.142
Mean ± SD	1.984±0.003	0.263±0.006	0.387±0.011	0.148±0.006

CrCEST, CEST effect of Cr; CEST, chemical exchange saturation transfer; Cr, creatine; NMR, nuclear magnetic resonance; SD, standard deviation.

https://dx.doi.org/10.21037/qims-24-1228

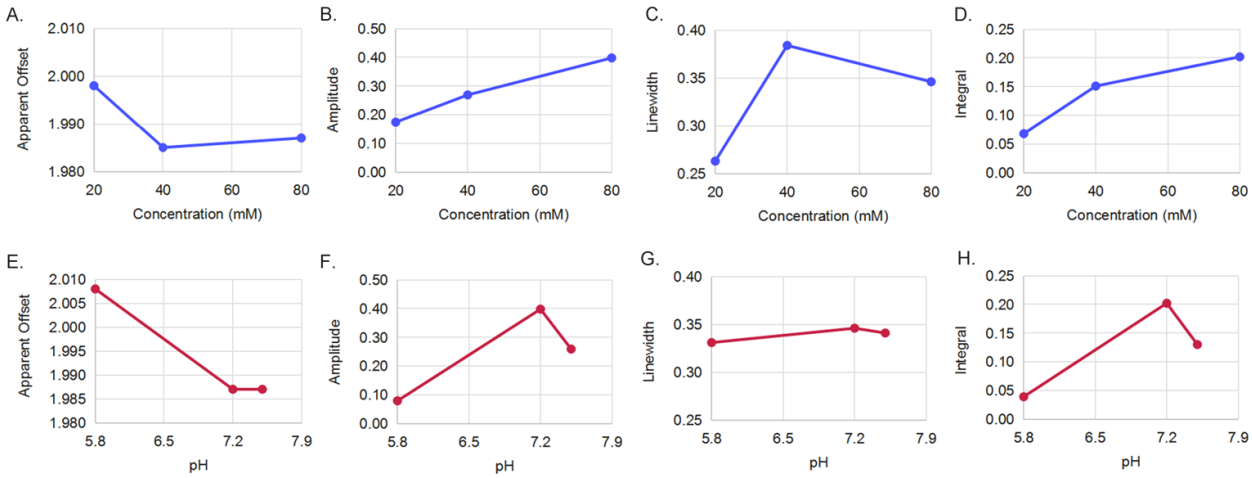

Figure S2 The apparent offset, amplitude, linewidth, and the integral values of CrCEST peaks in the Z-spectra of phantoms with different Cr concentrations and pH values. Experiments on a 400 MHz NMR spectrometer. CrCEST, CEST effect of Cr; CEST, chemical exchange saturation transfer; Cr, creatine; NMR, nuclear magnetic resonance.

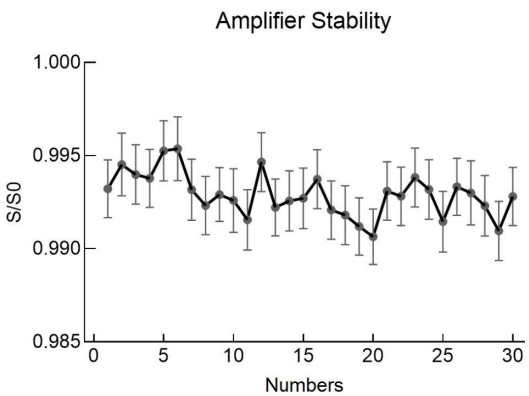

Figure S3 The CEST signals at −300 ppm for Cr phantom {[Cr] =80 mM and pH =6.6} that were repeatedly measured 30 times at 5.0 T MRI scanner under condition of the saturation time of 4 s and saturation power of 0.6 μT. CEST, chemical exchange saturation transfer; Cr, creatine; MRI, magnetic resonance imaging.

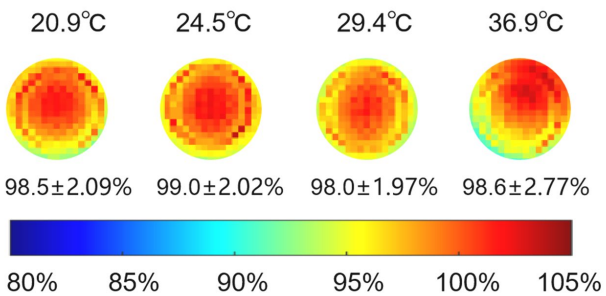

Figure S4 B_1 maps of Cr phantom {[Cr] =80 mM and pH =6.6} measured at different temperatures. Cr, creatine.

https://dx.doi.org/10.21037/qims-24-1228

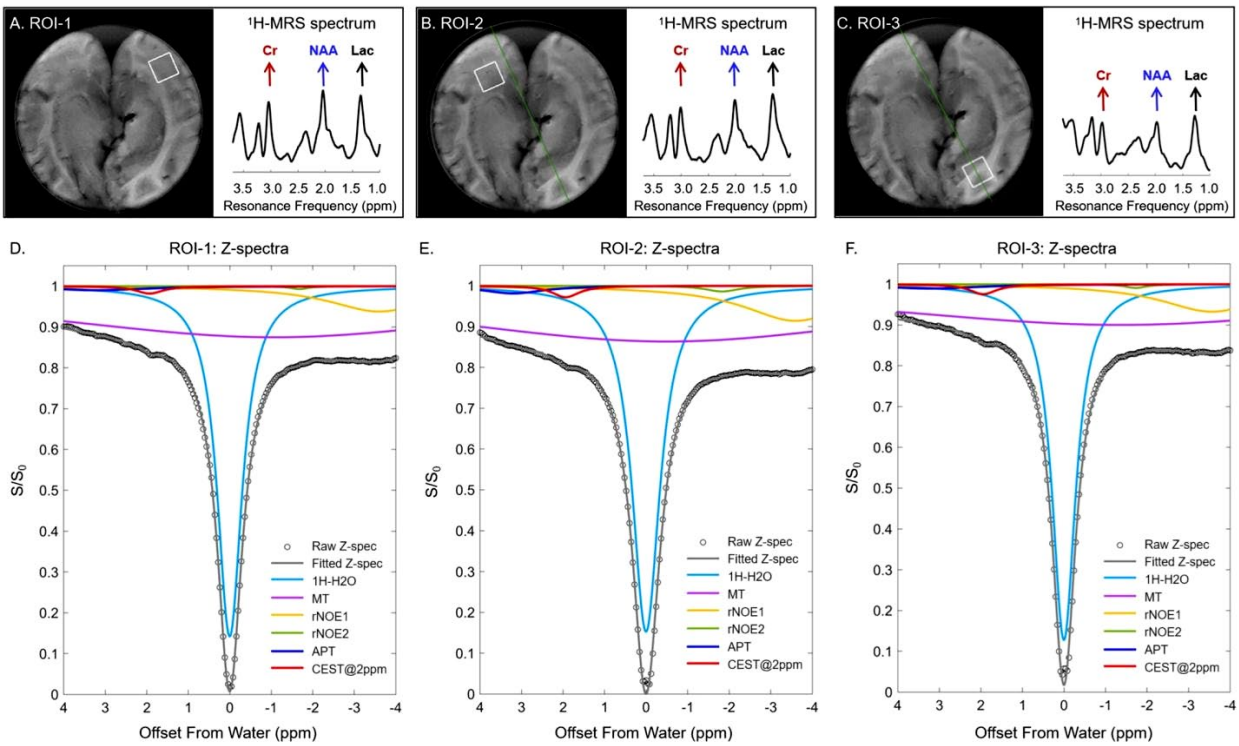

Figure S5 [1]H-MRS and CEST analyses of *ex vivo* swine brain immediately after sample preparation. (A-C) The [1]H-MRS spectra and (D-F) the Z-spectra of three isotropic VOIs in the swine brains measured immediately after samples preparation. The black circles and the gray line represent the raw and fitted Z-spectra, respectively. The light blue, purple, orange, green, dark blue, and red lines represent the fitted spectra of water, MT, rNOE@-3.5ppm, rNOE@-1.6ppm, APT, and CEST@2ppm, respectively. ROI, region of interest; [1]H-MRS, proton magnetic resonance spectroscopy; Cr, creatine; NAA, N-acetylaspartate; Lac, lactic acid; MT, magnetization transfer; rNOE, relayed nuclear Overhauser effect; APT, amide proton transfer; CEST@2ppm, CEST signal at 2 ppm; CEST, chemical exchange saturation transfer; VOI, volume of interest; rNOE@-3.5ppm, rNOE signal at –3.5 ppm; rNOE@-1.6ppm, rNOE signal at –1.6 ppm.

https://dx.doi.org/10.21037/qims-24-1228

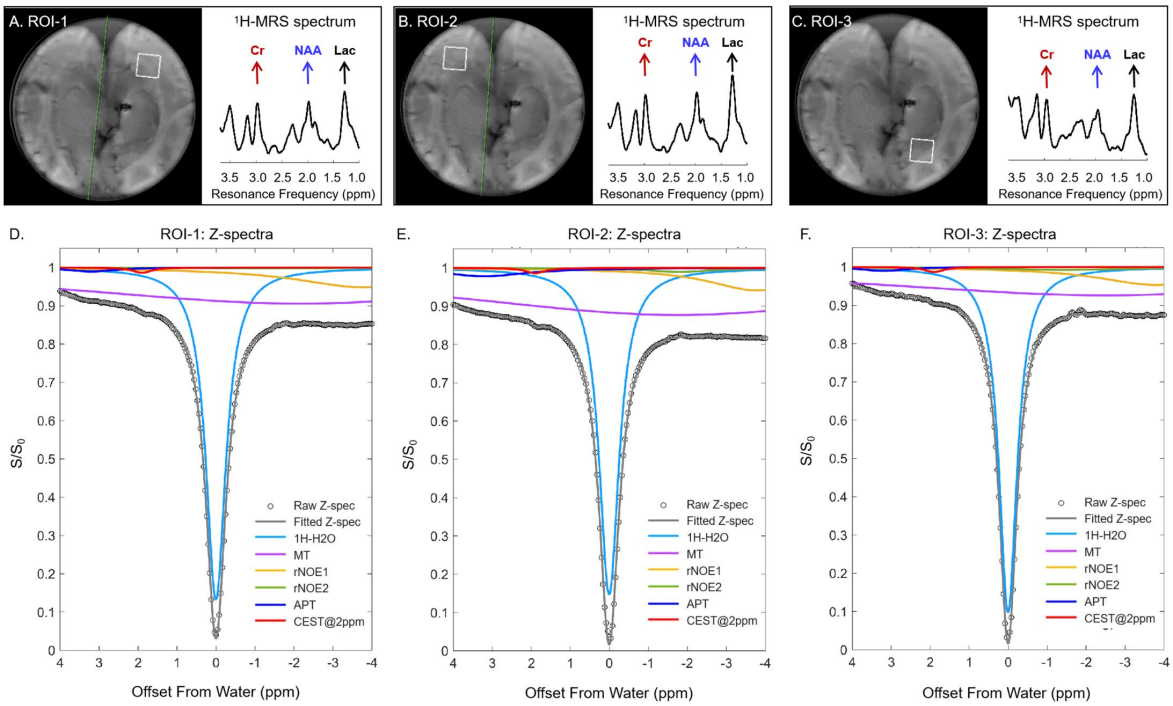

Figure S6 [1]H-MRS and CEST analyses of *ex vivo* swine brain at 9 hours after sample preparation. (A-C) The [1]H-MRS spectra and (D-F) the Z-spectra of three isotropic VOIs in the swine brains measured at the 9[th] hours after sample preparation. The black circles and the gray line represent the raw and fitted Z-spectra, respectively. The light blue, purple, orange, green, dark blue, and red lines represent the fitted spectra of water, MT, rNOE@-3.5ppm, rNOE@-1.6ppm, APT, and CEST@2ppm, respectively. ROI, region of interest; [1]H-MRS, proton magnetic resonance spectroscopy; Cr, creatine; NAA, N-acetylaspartate; Lac, lactic acid; MT, magnetization transfer; rNOE, relayed nuclear Overhauser effect; APT, amide proton transfer; CEST@2ppm, CEST signal at 2 ppm; CEST, chemical exchange saturation transfer; VOI, volume of interest; rNOE@-3.5ppm, rNOE signal at –3.5 ppm; rNOE@-1.6ppm, rNOE signal at –1.6 ppm.

https://dx.doi.org/10.21037/qims-24-1228

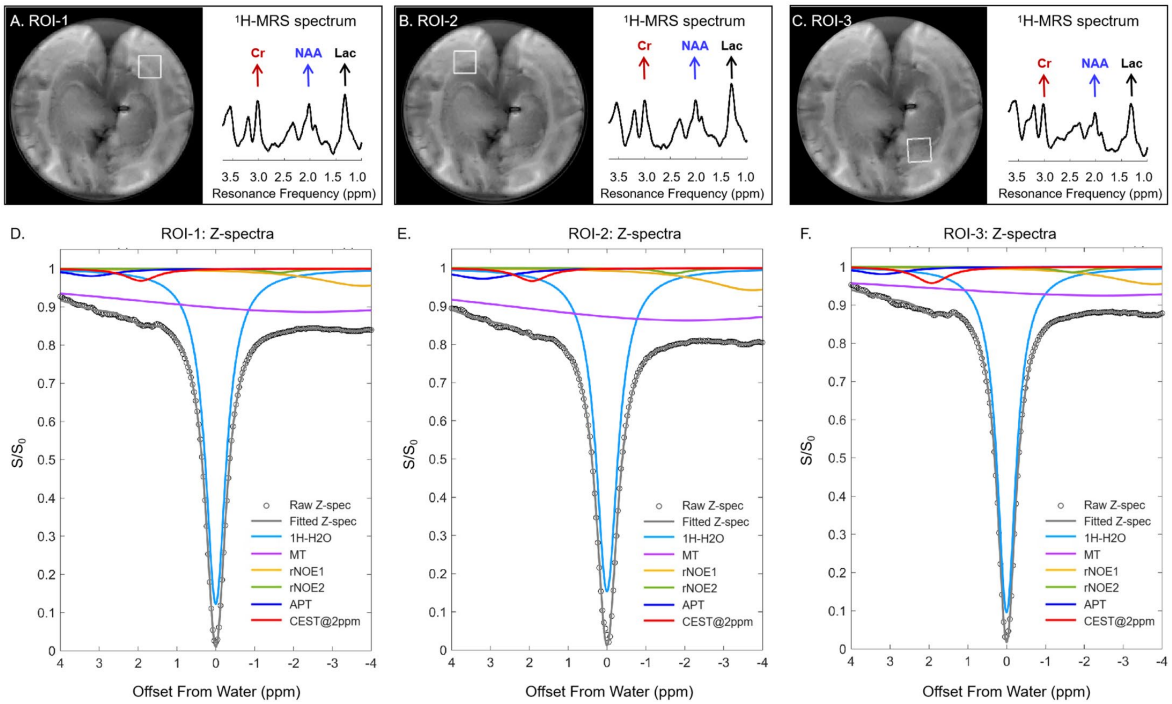

Figure S7 [1]H-MRS and CEST analyses of *ex vivo* swine brain at 12 hours after sample preparation. (A-C) The [1]H-MRS spectra and (D-F) the Z-spectra of three isotropic VOIs in the swine brains measured at the 12[th] hours after sample preparation. The black circles and the gray line represent the raw and fitted Z-spectra, respectively. The light blue, purple, orange, green, dark blue, and red lines represent the fitted spectra of water, MT, rNOE@-3.5ppm, rNOE@-1.6ppm, APT, and CEST@2ppm, respectively. ROI, region of interest; [1]H-MRS, proton magnetic resonance spectroscopy; Cr, creatine; NAA, N-acetylaspartate; Lac, lactic acid; MT, magnetization transfer; rNOE, relayed nuclear Overhauser effect; APT, amide proton transfer; CEST@2ppm, CEST signal at 2 ppm; CEST, chemical exchange saturation transfer; VOI, volume of interest; rNOE@-3.5ppm, rNOE signal at –3.5 ppm; rNOE@-1.6ppm, rNOE signal at –1.6 ppm.

https://dx.doi.org/10.21037/qims-24-1228

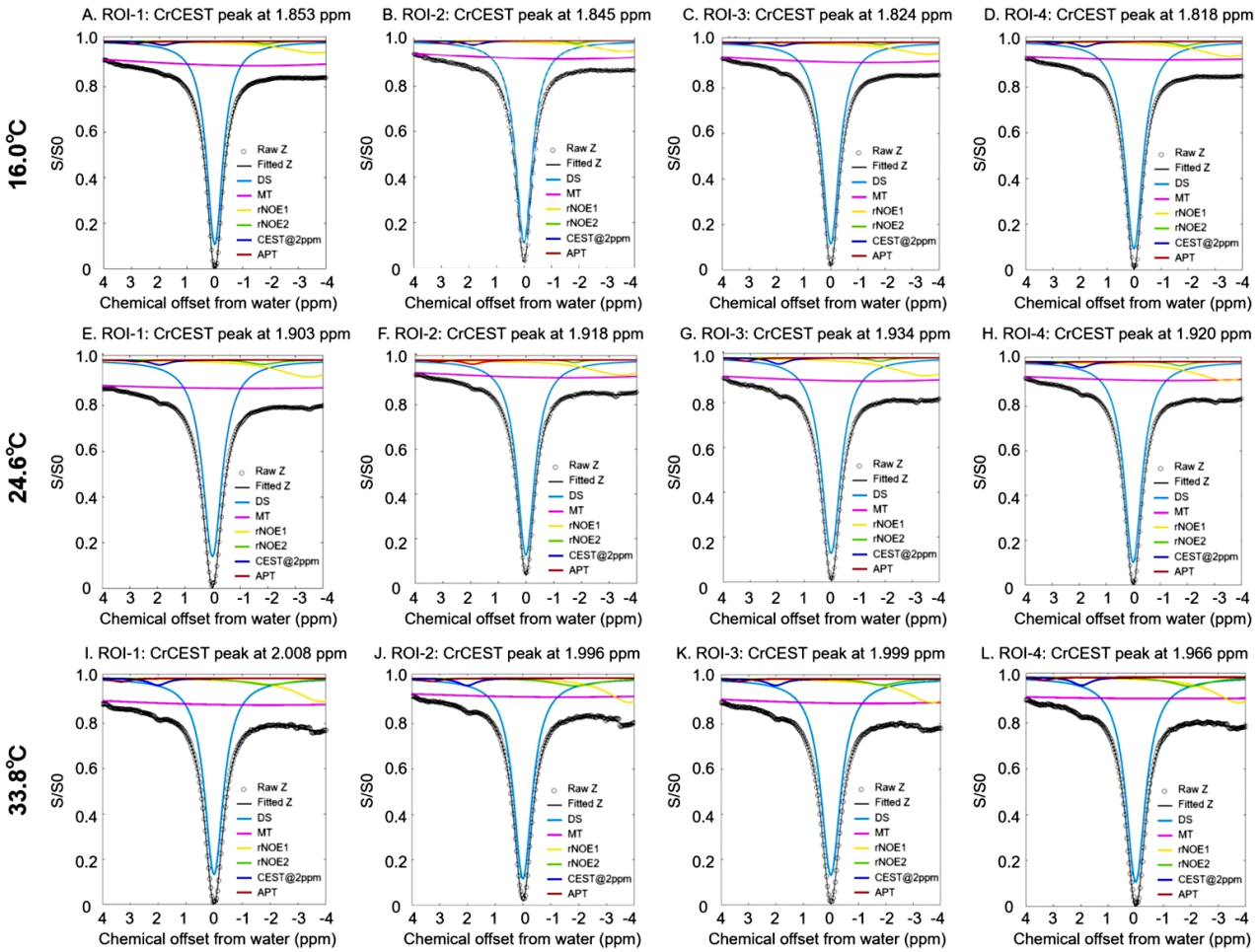

Figure S8 Fitted Z-spectra of ROIs within swine brains obtained at three different temperatures on a 5.0 T MRI scanner. The spatial locations of the four ROIs were depicted in *Figure 6*. The black circles and the gray line represent the raw and fitted Z-spectra, respectively. The light blue, purple, orange, green, dark blue, and red lines represent the fitted spectra of water, MT, rNOE@-3.5ppm, rNOE@-1.6ppm, APT, and CEST@2ppm, respectively. ROI, region of interest; CrCEST, CEST effect of Cr; CEST, chemical exchange saturation transfer; Cr, creatine; DS, direct water saturation; MT, magnetization transfer; rNOE, relayed nuclear Overhauser effect; CEST@2ppm, CEST signal at 2 ppm; APT, amide proton transfer; rNOE@-3.5ppm, rNOE signal at –3.5 ppm; rNOE@-1.6ppm, rNOE signal at –1.6 ppm.

https://dx.doi.org/10.21037/qims-24-1228

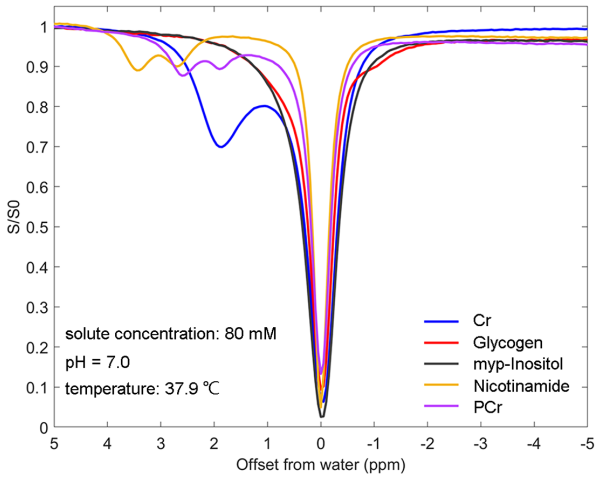

Figure S9 Z-spectra of Cr (blue line), glycogen (red line), myo-inositol (black line), nicotinamide (orange line), and PCr (purple line) phantoms with a solute concentration of 80 mM and pH of 7.0, which were measured with a CW CEST sequence (saturation time of 4 s and B_1 of 0.6 μT) at 37.9 ℃ at 5.0 T MRI scanner. Cr, creatine; PCr, phosphocreatine; CW, continuous wave; CEST, chemical exchange saturation transfer; MRI, magnetic resonance imaging.

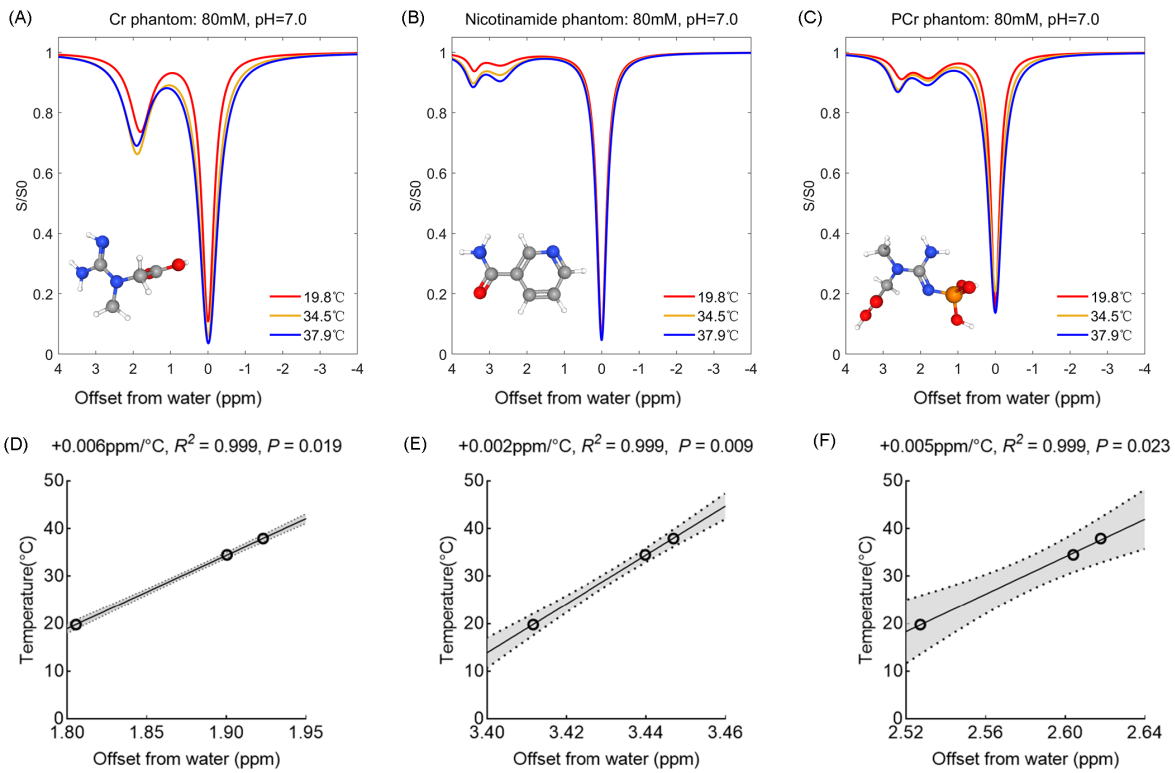

Figure S10 Temperature dependency of the apparent chemical shifts of Cr, nicotinamide and PCr. (A-C) Z-spectra and molecular structures of Cr, nicotinamide, and PCr phantoms with concentration of 80 mM and pH of 7.0 were measured with a CW CEST sequence (saturation time of 4 s and B_1 of 0.6 μT) at 19.8 ℃ (red line), 34.5 ℃ (orange line), and 37.9 ℃ (blue line) using 5.0 T MRI. (D-F) The temperature dependency coefficients of the exchangeable protons of Cr (Guan proton at around 1.9 ppm), nicotinamide (amine protons at around 3.4 ppm), and PCr (amide proton at around 2.6 ppm). Cr, creatine; PCr, phosphocreatine; CW, continuous wave; CEST, chemical exchange saturation transfer; MRI, magnetic resonance imaging; Guan, guanidinium.

https://dx.doi.org/10.21037/qims-24-1228

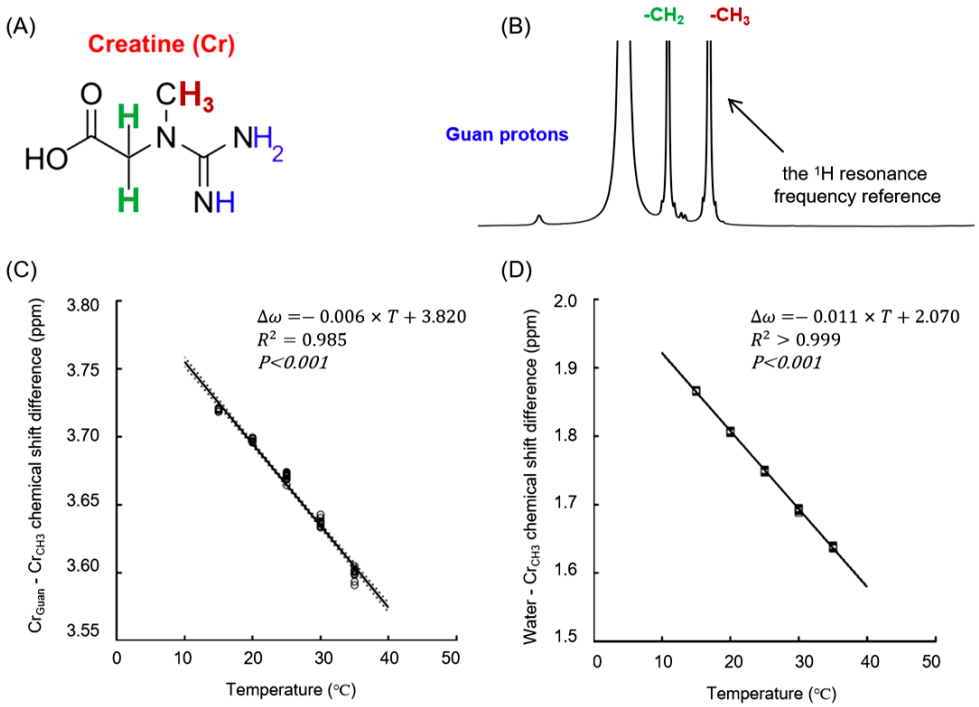

Figure S11 Temperature dependency of the MR frequency of Cr-Guan observed in the 500 MHz NMR experiments. Conditions: [Cr] =80 mM, 99% D_2O, pH =7.2, 15~35 ℃. (A) Chemical structure depiction of Cr. (B) ^{1}H-NMR spectrum of Cr at 20 ℃. (C) The linear correlation between temperature and the resonance frequency of Cr-Guan relative to the methyl group of Cr (Cr-CH_3) as the internal reference. (D) The linear correlation between temperature and the ^{1}H resonance frequency of water with Cr-CH_3 as the MR frequency reference. Cr, creatine; Guan, guanidinium; MR, magnetic resonance; Cr-Guan, guanidinium protons of Cr; NMR, nuclear magnetic resonance.

https://dx.doi.org/10.21037/qims-24-1228